A Genome-Wide Association Study Reveals a Novel Regulator of Ovule Number and Fertility in *Arabidopsis thaliana*

Jing Yuan[1,2] and Sharon A. Kessler[1,2*]

[1]Department of Botany and Plant Pathology, Purdue University, West Lafayette, Indiana USA

[2]Purdue Center for Plant Biology, Purdue University, West Lafayette, Indiana USA

* Corresponding author
Email: sakessler@purdue.edu

Short title

Regulation of ovule number in Arabidopsis

Abstract

Ovules contain the female gametophytes which are fertilized during pollination to initiate seed development. Thus, the number of ovules that are produced during flower development is an important determinant of seed crop yield and plant fitness. Mutants with pleiotropic effects on development often alter the number of ovules, but specific regulators of ovule number have been difficult to identify in traditional mutant screens. We used natural variation in Arabidopsis accessions to identify new genes involved in the regulation of ovule number. The ovule numbers per flower of 189 Arabidopsis accessions were determined and found to have broad phenotypic variation that ranged from 39 ovules to 84 ovules per pistil. Genome-Wide Association tests revealed several genomic regions that are associated with ovule number. T-DNA insertion lines in candidate genes from the most significantly associated loci were screened for ovule

number phenotypes. The *NEW ENHANCER of ROOT DWARFISM (NERD1)* gene was found to have pleiotropic effects on plant fertility that include regulation of ovule number and both male and female gametophyte development. Overexpression of NERD1 increased ovule number per fruit in a background-dependent manner and more than doubled the total number of flowers produced in all backgrounds tested, indicating that manipulation of NERD1 levels can be used to increase plant productivity.

Author Summary

Ovules are the precursors of seeds in flowering plants. Each ovule contains an egg cell and a central cell that fuse with two sperm cells during double fertilization to generate seeds containing an embryo and endosperm. The number of ovules produced during flower development determines the maximum number of seeds that can be produced by a flower. In this paper, we used natural variation in *Arabidopsis thaliana* accessions to identify regions of the genome that are associated with ovule number. Polymorphisms in the plant-specific NERD1 gene on chromosome 3 were significantly associated with ovule number. Mutant and overexpression analyses revealed that *NERD1* is a positive regulator of ovule number, lateral branching, and flower number in Arabidopsis. Manipulation of NERD1 expression levels could potentially be used to increase yield in crop plants.

Key Words

Ovule number, NERD1, Arabidopsis, Branching, Carpel Margin Meristem, GWAS

Introduction

During plant reproduction, pollen tubes deliver two sperm cells to female gametophytes contained within ovules. This allows double fertilization to occur in order to produce the embryo and endosperm in the developing seed. Angiosperms with all kinds of pollination syndromes (insect-, wind-, and self-pollinated) produce much more pollen than ovules in order to ensure successful pollination. For example, most soybean varieties produce only 2 ovules per flower, but more than 3,000 pollen grains, a 1,500-fold difference(1). Wind-pollinated plants such as maize have an even more extreme difference in pollen production vs. ovule production per plant, with more than 1 million pollen grains versus an average of 250 ovules per plant (a 4000-fold difference(2)). *Arabidopsis thaliana*, which is a self-pollinating plant, also produces an excess of pollen, with at least 2000 pollen grains per flower compared to an average of 60 ovules per flower(3). Since pollen is produced in excess, in self-pollinated plants the number of ovules (i.e. female gametes) sets the maximum seed number per flower.

The ability to manipulate ovule number to increase the reproductive potential of plants requires an understanding of the molecular pathways that control ovule initiation. The model plant *Arabidopsis thaliana* produces flowers with four whorls of organs: sepals, petals, stamens, and carpels. The inner whorls (3 and 4) are responsible for sexual reproduction, with pollen (the male gametophytes) produced in the whorl 3 stamens and the female gametophytes (also known as the embryo sacs), produced in ovules contained within the whorl 4 carpels. Specification of the 4 whorls is controlled by

74 the “ABC” genes, with the C-class gene AGAMOUS (AG) a major regulator of carpel
75 development(4).
76
77 In Arabidopsis, ovules are initiated from the carpel margin meristem (CMM) at stage 9
78 of floral development(5). The Arabidopsis gynoecium comprises two carpels that are
79 fused vertically at their margins (6). The CMM develops on the adaxial face of the
80 carpels (inside the fused carpel cylinder) and will give rise to the placenta, ovules,
81 septum, transmitting tract, style, and stigma. Once the placenta is specified, all of the
82 ovule primordia are initiated at the same time(7). Subsequently, each primordium will be
83 patterned into three different regions: the funiculus, which connects the ovule to the
84 septum; the chalaza, which gives rise to the integuments; and the nucellus, which gives
85 rise to the embryo sac. Ovule development concludes with the specification of the
86 megaspore mother cell within the nucellus which undergoes meiosis followed by three
87 rounds of mitosis to form the mature haploid embryo sac (reviewed in(8)).
88
89 In Arabidopsis, CMM development requires coordination of transcriptional regulators
90 involved in meristem function with hormone signaling (reviewed in(6)). Most mutants
91 that have been reported to affect ovule number have pleiotropic effects related to the
92 establishment of polarity and boundaries during gynoecial development (reviewed in
93 (9)). For example, the *AINTEGUMENTA* (*ANT*) transcription factor regulates organ
94 initiation and cell divisions during flower development(10). *ANT* acts redundantly with
95 the related gene *AINTEGUMENTA-LIKE6/PLETHORA3* to regulate carpel margin
96 development and fusion which leads to a modest reduction in ovule number. This

97 phenotype is exacerbated when *ant* is combined with mutations in other carpel
98 development transcriptional regulators, such as *SEUSS* (*SEU*), *LEUNIG* (*LUG*),
99 *SHATTERPROOF1* and *2* (*SHP1* and *SHP2*), *CRABSCLAW* (*CRC*), *FILAMENTOUS*
100 *FLOWER* (*FIL*), and *YABBY3* (*YAB3*). Mutant combinations between *ant* and these
101 mutants leads to severe defects in carpel fusion coupled with severe reductions in the
102 marginal tissues that give rise to the CMM (summarized in(6)). An extreme example is
103 the double mutant *seu-3 ant-1* which results in a complete loss of ovule initiation due to
104 defects in CMM development(11). The organ boundary genes, *CUP-SHAPED*
105 *COTYLEDON1* and *2* (*CUC1* and *CUC2*), are also required for CMM development and
106 subsequent ovule initiation. *ant cuc2* mutants with *cuc1* levels decreased specifically in
107 the CMM by an RNAi construct driven by the *SEEDSTICK* promoter show an 80%
108 reduction in ovule number, indicating that *ANT* controls cell proliferation while *CUC1/2*
109 are necessary to set up the boundaries that allow ovule primordia to be initiated(12).

110 Plant hormones are also involved in gynoecium development and can have both indirect
111 and direct effects on ovule number. Auxin biosynthesis, transport, signaling, and
112 transport mutants have varying effects on gynoecium development and patterning,
113 many of which lead to pleiotropic effects on tissues and organs derived from the
114 CMM(13). Treatment of developing flowers with the auxin polar transport inhibitor NPA
115 showed that an apical-basal auxin gradient in the developing gynoecium is necessary
116 for patterning events that lead to ovule initiation(13). Cytokinin has also been implicated
117 in ovule initiation and development in Arabidopsis. Notably, triple mutants in the
118 *ARABIDOPSIS HISTIDINE KINASE* (*AHK*) cytokinin receptors, *AHK2*, *AHK3*, and
119 *AHK4/CRE1*, displayed a 90% reduction in ovule number due to decreased cytokinin

120 signaling(14). Conversely, double mutants in the cytokinin degrading cytokinin
121 oxidases/dehydrogenases (CKXs) displayed higher cytokinin levels in inflorescences
122 and produced more than double the number of ovules as in wild-type controls(15).
123 Brassinosteroids (BR) may also be positive regulators of ovule initiation. Gain-of-
124 function mutants in the BR-induced transcription factor *BZR1* had increased ovule
125 number per flower while BR-deficient and insensitive mutants had decreased ovule
126 number compared to wild-type controls. Upregulation of the ovule regulators *ANT* and
127 *HULLENLOS* (*HUL*) was correlated with *BZR1* activity, indicating the BR signaling
128 positively regulates ovule development(16). Recently, gibberellins were shown to
129 negatively regulate ovule number independently of auxin transport and signaling. A
130 gain-of-function mutation in the DELLA gene, GA-INSENSITVE (GAI) and loss-of-
131 function mutations in GA receptors all led to increased ovule number in Arabidopsis
132 (17).

133 To date, research on the factors controlling ovule number has been dominated by the
134 analyses of mutants that have been identified based on pleiotropic effects on
135 gynoecium development. In an attempt to identify loci that regulate ovule number
136 without affecting other aspects of flower morphology, we took advantage of natural
137 variation in ovule number in Arabidopsis accessions from diverse geographical
138 locations. Over 7,000 natural accessions are now available with intraspecific variation,
139 and next generation sequencing has been used to generate data on single nucleotide
140 polymorphisms (SNPs) from over 1,000 of these accessions as part of the 1001
141 genomes project(18). 100s of different phenotypes have been analyzed in this collection
142 such as flowering time, leaf shape and size, the ability to resist to pathogens, etc.(19).

143 In this study, we identified variation in ovule number per flower in a screen of 189
144 Arabidopsis accessions and conducted a Genome Wide Association Study (GWAS) to
145 identify loci associated with the ovule number trait. Further analysis of two loci identified
146 in our GWAS revealed that the *NEW ENHANCER of ROOT DWARFISM* (*NERD1*) and
147 *OVULE NUMBER ASSOCIATED 2* (*ONA2*) genes participate in the determination of
148 ovule number during Arabidopsis flower development. The discovery of new ovule
149 number regulators in Arabidopsis has the potential to provide targets for the
150 development of crop varieties with greater yield.
151

152 **Results**

153 **Natural Variation in Ovule Number**

154 We set out to identify new regulators of ovule number in Arabidopsis by taking
155 advantage of phenotypic variation in naturally occurring accessions. We obtained 189
156 Arabidopsis accessions from the ABRC and assayed them for variation in ovule number
157 (Table S1). Since ovule number can vary throughout the life cycle of the plant(20), we
158 determined the average number of ovules from flowers 6-10 on the main stem of plants
159 that were vernalized for 4 weeks and then grown in long days at 22˚C. Under these
160 growth conditions, accessions displayed a remarkable diversity in ovule number per
161 flower, with a range of 39-82 ovules per flower (Fig 1A-B). The commonly used
162 reference accession, Col-0, falls in the middle of the range with an average ovule
163 number of 63±3 ovules.
164

165 In contrast to flowering time variation which has been shown to correlate with latitude of
166 origin in Arabidopsis accessions(21), ovule number was not strongly correlated with
167 location of origin in the accessions analyzed (Fig 1C, S1). Mapping ovule number data
168 onto a cladogram of the accessions used in our study revealed a cluster of low ovule
169 number accessions in one specific clade, indicating that these closely-related
170 accessions may have similar genetic control of ovule number (Fig 1D). Interestingly,
171 several clades were made up of accessions with high, medium, and low ovule numbers.
172 This suggests that the ovule number trait may be regulated by different loci that have
173 been selected for in some lineages.
174
175 **GWAS reveals SNPs linked to natural variation in ovule number**
176 In order to identify genomic regions linked to variation in ovule number, we assessed
177 whether the average ovule number per flower from 148 accessions was predicted by
178 Single Nucleotide Polymorphisms (SNP) available in the 1001 Full-sequence dataset;
179 TAIR 9. Logarithmic transformation was applied to the ovule number data to make the
180 results more reliable for parametric tests. Associations were tested for each SNP using
181 a linear regression model (LM) and the results were analyzed using GWAPP(22) (Fig
182 2A). A significance cutoff value of $-\log_{10}(p \text{ values}) \geq 6.2$ identified at least 9 genomic
183 regions that are associated with variation in ovule number, while a higher cutoff of –
184 $\log_{10}(p \text{ values}) \geq 7.5$ identifies only four significant genomic regions.
185
186 We next determined if known ovule number regulators (9, 15, 17, 23) colocalized with
187 our GWAS loci. Of the previously described loci, only BIN2 mapped close to a

188 significant association (Fig S2). This indicates that our GWAS has identified novel
189 functions for loci in the regulation of ovule number. For further analysis, we focused on
190 the two loci with the lowest p-values which are both located on the long arm of
191 chromosome 3 (Fig 2B-C). Genes containing the most significantly associated SNPs as
192 well as the 10 surrounding genes around the highest peak were considered as
193 candidates for regulating ovule number. These genes were further prioritized based on
194 whether they are expressed in developing pistils, by examining publicly available
195 transcriptome data in ePlant(24) (Fig S3). Based on this prioritization, 35 candidate
196 genes were selected, and of these 26 insertion mutants were available from the
197 Arabidopsis Biological Resource Center. All 26 mutants were evaluated for changes in
198 ovule number compared to the wild-type background, Col-0 (Table S2). Of these, two
199 had significantly reduced ovule number compared to the Col-0 control (Fig 3A, S4). The
200 strongest ovule number phenotype was found in insertion mutants in At3g51050, a gene
201 that was recently identified in a screen for enhancers of exocyst-mediated root
202 phenotypes and named *NEW ENHANCER OF ROOT DWARFISM 1* (*NERD1*)(25). The
203 second locus with T-DNA insertions affecting ovule number identified in our screen was
204 At3g60660, which we call *OVULE NUMBER ASSOCIATED 2* (*ONA2)*. *ONA2* encodes
205 an unknown protein containing a DUF1395 domain (TAIR) (Fig 2C).
206

207 ***NERD1* is a positive regulator of ovule number**

208 We focused our analysis on *NERD1* since it had the strongest effect on ovule number.
209 The fruits of homozygous mutants in two T-DNA insertion alleles, *nerd1-2* (described in
210 (25) and *nerd1-4,* had fewer ovules than wild-type plants (Fig 3A). To confirm that this

211 resulted from the disruption of NERD1, we generated transgenic plants expressing a
212 translational fusion of the *NERD1* protein with the red-fluorescent protein tdTomato
213 under the control of the native *NERD1* promoter. In *nerd1-2* and *nerd1-4* mutants, this
214 transgene fully rescued the reduced ovule phenotype and resulted in plants with ovule
215 numbers indistinguishable from Col-0 (Fig 3A). This demonstrates that *NERD1* is a
216 positive regulator of ovule number.
217
218 In addition to reduced ovule number per flower, homozygous *nerd1* mutants had fertility
219 defects. Homozygous *nerd1-2* mutants had 100% unfertilized ovules and homozygotes
220 of the less severe *nerd1-4* allele had 75% unfertilized ovules (Fig 3B-C and S5). *nerd1-*
221 *2* mutants displayed both male and female defects. No viable pollen grains were
222 produced (Fig 3D-E) and embryo sacs were often aborted, leading to 40% unfertilized
223 ovules in *nerd1-2/nerd1-2* plants pollinated with wild-type pollen (Fig 3F-G and S5). We
224 performed reciprocal crosses between heterozygous *nerd1-2* mutants and Col-0 to
225 determine if the fertility defects were gametophytic or sporophytic. When heterozygous
226 *nerd1-2/NERD1* was used as the female, there was no transmission defect,
227 demonstrating that the reduced female fertility in *nerd1-2* mutants was not
228 gametophytic. When *nerd1-2/NERD1* was used as the pollen donor, the transmission
229 efficiency of the mutant allele was reduced to 45%, indicating a male gametophytic
230 transmission defect (Table 1).

Table 1. Transmission efficiency of the *nerd1-2* allele determined by reciprocal crosses with wild-type Col-0.

Female	Male	*NERD1/ NERD1*	*nerd1-2/ NERD1*	Female TE%	Male TE %
nerd1-2/NERD1	Col-0	43	42	97.67	NA
Col-0	*nerd1-2/NERD1*	92	41	NA	44.57

231

232

233 ***NERD1* encodes an integral membrane protein**

234 Phylogenetic analyses indicate that *NERD1* is a member of a low-copy number, highly
235 conserved gene family that is found throughout the plant kingdom and in cyanobacteria
236 (Fig 4A-B and (25)). The NERD1 protein is predicted to be an integral membrane
237 protein with a signal peptide and one transmembrane domain (Fig 5A). The majority of
238 the protein is predicted to be extracellular, with the transmembrane domain located near
239 the C-terminus and a 17 amino acid cytoplasmic extension. Transient expression of a
240 NERD1-GFP fusion in *Nicotiana benthamiana* with subcellular markers confirmed that
241 NERD1 co-localizes with the Golgi marker and partially colocalizes with a plasma
242 membrane marker (Fig 5B and D). NERD1 does not co-localize with ER, peroxisome,
243 and plastid markers (Fig 5C and S6).

244

245 ***NERD1* is expressed throughout Arabidopsis development**

246 The *nerd1* ovule number and fertility phenotypes suggest that *NERD1* should be
247 expressed in developing flowers. We used a $NERD1_{pro}$*::gNERD1-GUS* fusion to
248 examine *NERD1* expression throughout Arabidopsis development. In
249 $NERD1_{pro}$*::gNERD1-GUS* inflorescences, GUS activity was detected throughout flower
250 development, including inflorescences, developing and mature anthers, and in the

251 stigma, ovules, and carpel walls of mature pistils (Fig 6). NERD1-GUS activity was
252 present in the carpel margin meristem (CMM) in stage 9 flowers, where ovule initiation
253 occurs (Fig 6C and E). *NERD1* reporter expression in the CMM during pistil
254 development is consistent with a role for *NERD1* in ovule initiation. During seedling
255 development, the *NERD1-GUS* reporter was detected in shoot and root apical
256 meristems (SAM and RAM) and in the vasculature (Fig 6I).
257
258 **Overexpression of NERD1 increases plant productivity**
259 We examined *NERD1* transcript levels in the low ovule number accession Altai-5
260 compared to Col-0. *NERD1* transcript accumulation was reduced in Altai-5 buds as
261 compared to Col-0 but similar in Altai-5 and Col-0 leaves (Fig 7). We hypothesized that
262 the low ovule number in Altai-5 may be linked to reduced *NERD1* expression in
263 developing flowers. In order to determine whether increasing *NERD1* expression is
264 sufficient to increase ovule number, we transformed Col-0 and the low ovule number
265 accession Altai-5, with a *NERD1-GFP* fusion construct driven by the constitutively
266 expressed Cauliflower Mosaic Virus 35S promoter (*35S::NERD1-GFP*). Overexpression
267 of *NERD1* had no effect on ovule number in the Col-0 background, but significantly
268 increased ovule number in the Altai-5 background (Fig 8A-C), indicating that the *NERD1*
269 effect on ovule number is background-dependent. The *35S::NERD1-GFP* plants
270 displayed an even more striking phenotype when overall plant architecture was
271 examined (Fig 8A). In both the Altai-5 and Col-0 backgrounds, *NERD1* overexpression
272 led to increased branching (Fig 8D) and shortened internode lengths between flowers,
273 leading to an overall increase in flower number in the overexpression plants compared

274 to untransformed controls (Fig 8E-H). Thus, *NERD1* overexpression leads to increased
275 biomass and reproductive capacity, with up to a 2.5-fold increase in total flower number
276 over the lifespan of the plant. While all independent transformants displayed increased
277 branching and flower number, some of the *35S::NERD1* plants were male sterile (Fig
278 S7). This male sterility correlated with *NERD1* expression levels and plants with higher
279 *NERD1* transcript levels had more severe male sterility (Fig S7). The sterility effect was
280 more severe in Col-0 than in Altai-5 (Fig S7). The lower endogenous *NERD1*
281 expression in Altai-5 inflorescences might explain the lower sensitivity of Altai-5 to
282 *NERD1* overexpression with respect to male fertility, demonstrating background-
283 dependent sensitivity to *NERD1* levels for both ovule number and male sterility.
284
285 *NERD1* was recently identified in enhancer screen performed on exocyst mutants with
286 weakly dwarfed roots. *nerd1* mutants have reduced root growth as a result of impaired
287 cell expansion, indicating that NERD1 may be a positive regulator of exocyst-dependent
288 root growth(25). Consistently, the *35S::NERD1-GFP* plants had longer roots compared
289 to the Col-0 control, indicating that root development is also sensitive to *NERD1*
290 expression levels (Fig S8).
291
292 Three SNPs in NERD1 showed significant correlation with ovule number in our GWAS
293 (Fig 9A-B). Two of them are synonymous SNPs that are not predicted to change the
294 amino acid sequence, but the third is a non-synonymous SNP (C to A change in
295 comparison to Col-0 reference) causing a Serine to Tyrosine change at amino acid 230
296 of NERD1 (Fig 9A-B). This non-synonymous SNP was present in 10 out of the 16

297 lowest ovule number accessions and not present in the 16 highest ovule number
298 accessions (Fig 9A). Across all of the accessions in our GWAS panel, the “A” allele at
299 this position was significantly associated with lower ovule numbers (Fig 9C). However,
300 some accessions with the “C” allele of *NERD1* have low ovule numbers, including the
301 Altai-5 accession (Fig 9A), underscoring that multiple mechanisms influence ovule
302 number in Arabidopsis.
303

304 **Discussion**

305 Our experiments revealed that Arabidopsis displays a wide variation in the number of
306 ovules per flower, a key component of plant fitness and crop yield. Association genetics
307 linked this natural variation to the plant-specific gene, *NERD1*, that regulates the
308 number of ovules produced in Arabidopsis flowers and gametophyte development (Fig
309 3) and was previously found to alter root growth(25). Overexpression of *NERD1* led to
310 dramatic effects on plant architecture, indicating that *NERD1* may be involved in
311 regulating meristem activity during Arabidopsis development.
312

313 **GWAS reveals new ovule number-associated loci in Arabidopsis**

314 A quantitative trait locus (QTL) mapping study utilizing variation between L*er* and Cvi
315 identified QTLs residing on chromosomes 1, 2 (near the *ERECTA* gene), and two QTL
316 on chromosome 5(23). No follow-up study has identified the genes underlying these
317 QTLs. Our population displayed a much larger range of ovule numbers per flower (39-
318 84) than that seen in Cvi vs L*er* (66 and 56, respectively). We identified 9 significant
319 associations in our GWAS, but only one potentially overlaps with a known ovule number

320 QTL (see chromosome 5 in Fig S2). Of the genes with an identified effect on ovule
321 number, only BIN2 overlapped with a GWAS peak, indicating that our study has
322 revealed at least seven novel regulators of ovule number in Arabidopsis. We
323 molecularly identified two new genes that control ovule number that were linked to two
324 GWAS peaks on chromosome 3. This expands that number of known ovule number
325 determinants and confirms the value of GWAS as a forward genetics tool.
326
327 **NERD1 may transmit signals across membranes**
328 *NERD1* is a plant-specific, low copy number gene that is found throughout the plant
329 kingdom. NERD1 was recently identified as an enhancer of root development
330 phenotypes in weak mutants of the exocyst subunits SEC8 and EXO70A1(25) While a
331 direct interaction with the exocyst could not be identified, the authors identified Golgi
332 localization of NERD1 and hypothesized that NERD1 could be involved in synthesizing
333 or modifying pectins or other polysaccharide components of the cell wall that are
334 synthesized in the Golgi and transported to the cell wall (25). Changes in cell wall
335 elasticity mediated by pectin modifications have been correlated with lateral organ
336 initiation at the shoot apical meristem (26, 27). The decreased ovule number in *nerd1*
337 mutants and increased lateral branching and flower initiation in *35S::NERD1*
338 transformants could be consistent with alterations in Golgi-synthesized cell wall
339 components affecting cell wall mechanics and organ initiation.
340
341 Our GFP localization experiments confirmed Golgi localization of the majority of
342 NERD1-GFP, but also identified fluorescence in the plasma membrane. In Arabidopsis,

343 the NERD1 protein is predicted to encode a 698 amino acid protein with a signal
344 peptide, one transmembrane domain, and a short (17 amino acid) cytoplasmic tail at the
345 C-terminus. This topology is consistent with NERD1 being involved in transducing
346 signals from the outside of the cell to the inside, perhaps as part of a complex with other
347 membrane proteins. In animals, α-integrins and β-integrins share a similar topology with
348 NERD1 and interact with each other to transduce information from the extracellular
349 matrix to the inside of the cell(28). The existence of integrin-like complexes in plants
350 remains controversial, since plants lack proteins with clear sequence homology to
351 animal integrins. However, antibodies to animal β-integrins interact with plant proteins,
352 indicating structural conservation(29). NERD1 has a predicted beta-propeller with a
353 calcium-binding pocket similar to α-integrins in its extracellular domain(25), but
354 determination of whether NERD1 functions in an integrin-like fashion awaits further
355 investigation.
356
357 NERD1 could also interact with other types of proteins to transduce signals. In plants,
358 receptor-like proteins (RLPs) with short cytoplasmic domains have been shown to
359 heterodimerize with receptor-like kinases (RLKs) to form a receptor complex that
360 transduces extracellular signals to intracellular signaling networks. The Arabidopsis
361 genome contains 57 RLPs with Leucine Rich Repeats (LRRs) in their extracellular
362 domains(30). These LRR-RLPs have a transmembrane domain near the C-terminus
363 and a short cytoplasmic domain and are predicted to form complexes with LRR-RLKs.
364 LRR-RLP/LRR-RLK complexes have been implicated in plant growth and development
365 and plant immunity (reviewed in(31)). For example, the CLAVATA2 (CLV2) RLP forms a

366 complex with the RLKs CORYNE (CRN) and/or CLAVATA1 (CLV1) RLK to perceive the
367 CLAVATA3 (CLV3) ligand and trigger intracellular signaling related to shoot apical
368 meristem maintenance(32-34). Likewise, the TOO MANY MOUTHS (TMM) RLP
369 interacts with the LRR-RLKs ERECTA (ER) and ERECTA-LIKE1 (ERL) to regulate
370 stomatal patterning(35, 36). In contrast to the LRR-RLPs, NERD1 does not share
371 sequence homology with other proteins in the Arabidopsis genome. Distinguishing
372 whether NERD1 functions similarly to RLPs, integrins, or some other signaling network
373 will require identification of NERD1-interacting proteins in future work.
374
375 ***NERD1* and fertility**
376 Homozygous *nerd1* mutants are completely male sterile are partially female sterile. This
377 sterility is due to a lack of pollen production and problems in female gametophyte
378 development leading to aborted embryo sacs. Transmission efficiency tests using
379 heterozygous loss-of-function mutants revealed that *nerd1* could be transmitted through
380 the egg at near 100% efficiency, indicating a sporophytic effect on female gametophyte
381 development. Ovule development mutants that have defective integument development
382 such as *short integuments 1* (*sin1*), *bell 1* (*bel1*) and *ant* fail to produce functional
383 female gametophytes, indicating that female gametophyte development is dependent
384 on properly differentiated sporophytic cells in the ovule(37-41). Sporophytic
385 development in ovules seem to be normal in *nerd1* mutants, yet embryo sacs abort. As
386 a membrane protein, NERD1 could transmit some unknown signal between sporophytic
387 and gametophytic cells during embryo sac development.
388

389 The male fertility defect in *nerd1* plants is more severe than the female defect.
390 Homozygous *nerd1* anthers are empty, indicating that pollen development is not
391 initiated or aborted very early. Transmission efficiency tests using pollen from
392 heterozygous *nerd1* plants crossed to wild-type females revealed that *nerd1* also has
393 gametophytic effects on pollen function. The sporophytic effects could be related to
394 early stages of anther development. In particular, specification of the tapetum is critical
395 for pollen development (reviewed in(42)). In our *35S::NERD1* experiment, transformants
396 that accumulated the most *NERD1* transcripts were male sterile. Together these results
397 indicate that pollen development is sensitive to *NERD1* levels, i.e. either too much or
398 too little *NERD1* is detrimental to pollen development. Future experiments should focus
399 on determining the stage of anther and/or pollen development that is affected in *nerd1*
400 mutants and the specific cell types that express *NERD1* in developing anthers.
401
402 Even though *NERD1* is expressed broadly throughout the plant, above ground
403 vegetative development appears to be normal in *nerd1* loss-of-function mutants.
404 However, *nerd1* roots are shorter than normal and have root hair defects that include
405 bulging and rupture(25). *NERD1* could have distinct or related developmental functions
406 in roots and flowers, as is seen for many of the genes involved in hormonal regulation of
407 development(43).
408
409 ***NERD1* regulates lateral organ formation**
410 *NERD1* overexpression under control of the constitutive 35S promoter dramatically
411 changed plant architecture in both the Col-0 and Altai-5 backgrounds. *NERD1*

412 overexpression plants produced significantly more branches than wild-type controls and
413 produced significantly more flowers that were produced at closer intervals along the
414 stem. Like branches and flowers, ovules are lateral organs produced from meristematic
415 cells, indicating that *NERD1* may be a positive regulator of meristem activity. Lateral
416 meristem activation and subsequent branching have been shown to be affected by
417 several different hormones (reviewed in(44)). Classic experiments in *Vicia faba* showed
418 that auxin produced in the shoot apex inhibits axillary meristems(45), and more recently
419 strigolactones were identified as graft-transmissible suppressors of branching (reviewed
420 in (46)). Gibberellins also repress shoot branching in Arabidopsis, maize, and rice, with
421 GA-deficient mutants displaying increased branching compared to wild-type controls(47-
422 50). In contrast, cytokinins and brassinosteroids are both positive regulators of
423 branching(49-53). The mechanism through which these plant hormones work together
424 to regulate branching is unknown, but auxin has been proposed to control cytokinin and
425 strigolactone biosynthesis(54, 55), while the brassinosteroid signaling regulator *BES1*
426 may inhibit strigolactone signaling to promote branching(56). The promotion of
427 branching in *35S::NERD1* plants could be related to regulation of one or more of these
428 hormonal pathways. Like *NERD1*, upregulation of both cytokinin and brassinosteroid
429 signaling pathways have been shown to positively regulate branching and ovule
430 number(15, 53, 56, 57), suggesting that *NERD1* may be intimately connected to these
431 pathways. Future research is needed to explore the intersection between *NERD1* and
432 hormonal pathways.
433
434 ***NERD1*-induced increases in ovule number are background-dependent**

435 Overexpression of *NERD1* in the Col-0 and Altai-5 backgrounds led to increased
436 branching and flower number, but ovule number was only increased in the Altai-5
437 background, suggesting a background-dependence on the ovule number trait. In
438 Arabidopsis, natural accessions were shown to respond differently in their ability to
439 buffer GA perturbations caused by overexpressing GA20 oxidase 1, which encodes a
440 rate-limiting enzyme for GA biosynthesis(58). Genetic background dependence has
441 been shown to be a wide-spread phenomenon in *C. elegans*, with approximately 20% of
442 RNAi-induced mutations (out of 1400 genes tested) displaying different phenotypic
443 severity in two different genetic backgrounds(59). Similar to our results with *NERD1*,
444 where Altai-5 has lower endogenous levels of the *NERD1* transcript in developing
445 flowers compared to Col-0, the severity of the *C. elegans* phenotypes could be linked to
446 gene expression levels of either the target gene itself or other genes in the same
447 pathway(59).
448
449 Our GWAS revealed multiple novel loci that control ovule number in Arabidopsis. It
450 remains to be seen if exocyst function is linked to NERD1's role in ovule number
451 determination. Identification of NERD1 interacting proteins will provide candidates for
452 other players in the NERD1 pathway. Some of the other novel loci identified in our
453 GWAS may well participate in the same signaling pathway as *NERD1*. While *NERD1* is
454 a promising candidate for engineering plants with increased ovule number, the
455 differential responses to *NERD1* overexpression seen in Altai-5 and Col-0 suggest that
456 specific alleles at other loci may be necessary for achieving maximum effect of *NERD1*
457 overexpression.

458

459 **Materials and Methods**

460 **Plant Material and Growth Conditions**

461 *Arabidopsis thaliana* accessions and insertion mutants were ordered from the
462 Arabidopsis Biological Resource Center at Ohio State University (ABRC). ABRC stock
463 numbers for the accessions and insertion mutants used in our study are listed in
464 supplementary tables 1 and 2. Seeds were sterilized and plated on ½ Murashige and
465 Skoog (MS) plates. All plates were sealed and stratified at 4 ˚C for two days, and then
466 transferred to the growth chamber (long day conditions, 16h of light and 8 h of dark at
467 22˚C) for germination and growth. After one-week, seedlings were transplanted to soil.
468 Many of the Arabidopsis accessions require vernalization for flowering(60), we therefore
469 chose to vernalize all of the accessions in our study for 4 weeks at 4 ˚C. After
470 vernalization, the plants were returned to the growth chamber and grown under the long
471 day conditions described above. Seeds from transformed lines were sterilized and
472 plated on ½ MS plate with 20mg/L hygromycin for selection of transgenic seedlings,
473 which were then transplanted to soil and grown in long days.

474

475 **Ovule Number Phenotyping**

476 For determination of ovule number per flower, we counted four to five siliques per plant
477 and five plants per accession. Carpel walls were removed with a dissecting needle and
478 total ovule number (including unfertilized and aborted ovules) was counted with the aid
479 of a Leica dissecting microscope. To minimize age-related variation in ovule number,
480 we counted siliques from flowers 6-10 on the primary shoot for all accessions.

481

482 **Genome-Wide Association Study**

483 GWAS was performed using GWAPP, which is a GWAS web application for Genome-
484 Wide Association Mapping in *Arabidopsis* (http://gwas.gmi.oeaw.ac.at) (22). In our
485 study, 148 accessions had single nucleotide polymorphisms (SNPs) data available on
486 the 1001 Full-sequence dataset; TAIR 9. Logarithmic transformation was applied to
487 make the results more reliable for parametric tests. A simple linear regression (LM) was
488 used to generate the Manhattan plot by using GWAPP(22). SNPs with P values $\leq 1 \times$
489 10^{-6} were further considered as candidate loci linked to alleles that regulate ovule
490 number (a horizontal dashed line in Fig. 2 shows the 5% FDR threshold $-\log_{10}p$
491 value=6.2, which was computed by the Benjamini-Hochberg-Yekutieli method). SNPs
492 with <15 minor allele count (MAC) were not considered to help control false positive
493 rates. 10 genes flanking the highest SNP for each locus were tabulated as candidate
494 genes for each significant association.

495

496 **Cloning and Generation of Transgenic Lines**

497 For complementation and overexpression experiments, Gateway Technology was used
498 to make all the constructs. Genomic DNA fragments corresponding to the coding
499 regions of candidate genes were amplified from either beginning of the promoter
500 (defined by the end of the upstream gene) or the start codon to the end of the CDS
501 (without stop codon) by PCR with primers that had attB1 and attB2 sites from Col-0
502 genomic DNA (see supplementary table 3 for primer sequences). For amplifying
503 At3g60660 and At3g51050, PHUSION High-Fidelity Polymerase (NEB, M0535S) was

504 used. All the PCR products were put into entry vector pDONR207 by BP reactions and
505 then were recombined into destination vector pMDC83 (GFP) by LR reaction(61).
506 Native promoter constructs were amplified from ~2KB promoter region to the end
507 (without stop codon) by PCR with primers that had attB1 and attB2 sites from Col-0
508 genomic DNA. The PCR products were put into entry vector pDONR207 by BP
509 reactions and then were recombined into destination vector pMDC32 (tdTomato) and
510 pMDC163 (GUS) by LR reaction. All constructs were transformed into *Agrobacterium*
511 *tumefaciens* strain GV3101 and then used for plant transformation by the floral-dip
512 method(62).
513

514 **GUS Staining**

515 GUS staining was performed as previously described(63). Samples were imaged with
516 Differential Interference Contrast (DIC) on a Nikon Eclipse Ti2-E microscope. 12
517 independent T1 NERD-GUS transformants were analyzed and showed similar GUS
518 patterns.
519

520 **Transient Expression in *N. benthamiana***

521 Leaves from 3-4 week old *N. benthamiana* were co-infiltrated with 35S::NERD1-GFP
522 and Golgi-mCherry, ER-mCherry, PM-mCherry, Plastid- mCherry and Peroxisome-
523 mCherry markers from(64) as previously described(65). Leaves were imaged 2-3 days
524 after infiltration with a Nikon A1Rsi inverted confocal microscope under 20x dry and 40x
525 water objectives with GFP excited by a 488nm laser and mCherry excited by a 561nm
526 laser in normal mode.

527

528 **Alexander Staining of Pollen**

529 Mature anthers from Col-0 and *nerd1-2/nerd1-2* were dissected under the Leica
530 dissecting microscope and placed into a drop (20 µl) of Alexander staining solution on a
531 microscope slide(66). After several minutes of staining, samples were imaged with a
532 Nikon Eclipse Ti2-E microscope.

533

534 **Quantitative Real-time RT-PCR**

535 For qRT-PCR, leaves and young flowers were collected from mature plants of Col-0 and
536 Altai-5. Samples were immediately frozen in liquid nitrogen, ground, and total RNA was
537 extracted using the E.Z.N.A Plant RNA kit (OMEGA, USA). Oligo-dT primers and
538 Superscript II reverse transcriptase (Invitrogen) was used for cDNA synthesis. qRT-
539 PCR reactions were prepared using SYBR Green PCR Master Mix and PCR was
540 conducted with a StepOnePlus RT-PCR system. Relative quantifications were
541 performed for all genes with the Actin11 used as an internal reference. The primers
542 used for qRT-PCR shown in supplementary table 3.

543

544 **Phylogenetic Analysis**

545 The cladogram tree was generated in MEGA7, which nucleotide distance and neighbor-
546 join tree file were calculated by PHYlogeny Inference Package (PHYLIP, version 3.696).
547 The phylogenetic tree of NERD1 was inferred using neighbor-joining method in
548 MEGA7(67). The associated taxa clustered together with the bootstrap test (1000
549 replicates)(68). All the branch lengths are in the same units as those of the evolutionary

550 distances used to generate the phylogenetic tree.

551

552 **Supplemental Material**

553 **Supplementary Figure 1.** Statistical analysis of the association between geographic
554 distribution and ovule number per flower in the Arabidopsis accessions used in the
555 GWAS.

556 **Supplementary Figure 2.** Previously identified ovule number related genes' position in
557 relation to the Manhattan plot generated from the ovule number GWAS.

558 **Supplementary Figure 3.** Heat map of candidate gene expression patterns in
559 reproductive tissues.

560 **Supplementary Figure 4.** Average ovule number per flower of candidate gene T-DNA
561 mutants on chromosome 3.

562 **Supplementary Figure 5**. Homozygous *nerd1* mutants have high levels of infertility can
563 be partially rescued by pollinating with Col-0 wild-type pollen.

564 **Supplementary Figure 6.** Co-localization of 35S::NERD1-GFP with peroxisome and
565 plastid markers.

566 **Supplementary Figure 7.** Male sterility in *35S::NERD1* plants is linked to high *NERD1*
567 expression.

568 **Supplementary Figure 8.** *NERD1* is involved in in root growth.

569 **Supplementary Figure 9.** Amino acid changes in and around the *NERD1* gene in low
570 and high ovule number accessions.

571 **Supplementary table 1.** List of Arabidopsis accessions used in the study and their
572 ovule number data.

573 **Supplementary Figure 2.** Chromosome 3 candidate genes and insertion mutants.

574 **Supplementary Figure 3.** List of primers used for genotyping and cloning.

575

576 **References**

577 1. Palmer RG, Albertsen MC, Heer H. Pollen production in soybeans with respect to
578 genotype, environment, and stamen position. Euphytica. 1978;27(2):427-33.
579 2. Uribelarrea M, Cárcova J, Otegui ME, Westgate ME. Pollen Production,
580 Pollination Dynamics, and Kernel Set in Maize. Crop Science. 2002;42:1910-8.
581 3. Yan J, Chia JC, Sheng H, Jung HI, Zavodna TO, Zhang L, et al. Arabidopsis
582 Pollen Fertility Requires the Transcription Factors CITF1 and SPL7 That Regulate
583 Copper Delivery to Anthers and Jasmonic Acid Synthesis. Plant Cell. 2017;29(12):3012-
584 29.
585 4. Coen ES, Meyerowitz EM. The war of the whorls: genetic interactions controlling
586 flower development. Nature. 1991;353(6339):31-7.
587 5. Smyth DR, Bowman JL, Meyerowitz EM. Early Flower Development in
588 Arabidopsis. Plant Cell. 1990;2(8):755-67.
589 6. Reyes-Olalde JI, Zuniga-Mayo VM, Chavez Montes RA, Marsch-Martinez N, de
590 Folter S. Inside the gynoecium: at the carpel margin. Trends Plant Sci.
591 2013;18(11):644-55.
592 7. Robinson-Beers K, Pruitt RE, Gasser CS. Ovule Development in Wild-Type
593 Arabidopsis and Two Female-Sterile Mutants. Plant Cell. 1992;4(10):1237-49.
594 8. Drews GN, Koltunow AM. The female gametophyte. Arabidopsis Book.
595 2011;9:e0155.
596 9. Cucinotta M, Colombo L, Roig-Villanova I. Ovule development, a new model for
597 lateral organ formation. Front Plant Sci. 2014;5:117.
598 10. Klucher KM, Chow H, Reiser L, Fischer RL. The AINTEGUMENTA gene of
599 arabidopsis required for ovule and female gametophyte development is related to the
600 floral homeotic gene APETALA2. Plant Cell. 1996;8(2):137-53.
601 11. Azhakanandam S, Nole-Wilson S, Bao F, Franks RG. SEUSS and
602 AINTEGUMENTA mediate patterning and ovule initiation during gynoecium medial
603 domain development. Plant Physiol. 2008;146(3):1165-81.
604 12. Galbiati F, Sinha Roy D, Simonini S, Cucinotta M, Ceccato L, Cuesta C, et al. An
605 integrative model of the control of ovule primordia formation. Plant J. 2013;76(3):446-
606 55.
607 13. Nemhauser JL, Feldman LJ, Zambryski PC. Auxin and ETTIN in Arabidopsis
608 gynoecium morphogenesis. Development. 2000;127(18):3877-88.
609 14. Bencivenga S, Simonini S, Benkova E, Colombo L. The transcription factors
610 BEL1 and SPL are required for cytokinin and auxin signaling during ovule development
611 in Arabidopsis. Plant Cell. 2012;24(7):2886-97.
612 15. Bartrina I, Otto E, Strnad M, Werner T, Schmulling T. Cytokinin regulates the
613 activity of reproductive meristems, flower organ size, ovule formation, and thus seed
614 yield in Arabidopsis thaliana. Plant Cell. 2011;23(1):69-80.

615 16. Huang HY, Jiang WB, Hu YW, Wu P, Zhu JY, Liang WQ, et al. BR Signal
616 Influences Arabidopsis Ovule and Seed Number through Regulating Related Genes
617 Expression by BZR1. Molecular Plant. 2013;6(2):456-69.
618 17. Gomez MD, Barro-Trastoy D, Escoms E, Saura-Sanchez M, Sanchez I, Briones-
619 Moreno A, et al. Gibberellins negatively modulate ovule number in plants. Development.
620 2018;145(13).
621 18. Weigel D. Natural variation in Arabidopsis: from molecular genetics to ecological
622 genomics. Plant Physiol. 2012;158(1):2-22.
623 19. Atwell S, Huang YS, Vilhjalmsson BJ, Willems G, Horton M, Li Y, et al. Genome-
624 wide association study of 107 phenotypes in Arabidopsis thaliana inbred lines. Nature.
625 2010;465(7298):627-31.
626 20. Wetzsteini HY, Yi WG, Porter JA, Ravid N. Flower Position and Size Impact
627 Ovule Number per Flower, Fruitset, and Fruit Size in Pomegranate. J Am Soc Hortic
628 Sci. 2013;138(3):159-66.
629 21. Stinchcombe JR, Weinig C, Ungerer M, Olsen KM, Mays C, Halldorsdottir SS, et
630 al. A latitudinal cline in flowering time in Arabidopsis thaliana modulated by the flowering
631 time gene FRIGIDA. Proc Natl Acad Sci U S A. 2004;101(13):4712-7.
632 22. Seren U, Vilhjalmsson BJ, Horton MW, Meng D, Forai P, Huang YS, et al.
633 GWAPP: a web application for genome-wide association mapping in Arabidopsis. Plant
634 Cell. 2012;24(12):4793-805.
635 23. Alonso-Blanco C, Blankestijn-de Vries H, Hanhart CJ, Koornneef M. Natural
636 allelic variation at seed size loci in relation to other life history traits of Arabidopsis
637 thaliana. Proc Natl Acad Sci U S A. 1999;96(8):4710-7.
638 24. Waese J, Fan J, Pasha A, Yu H, Fucile G, Shi R, et al. ePlant: Visualizing and
639 Exploring Multiple Levels of Data for Hypothesis Generation in Plant Biology. Plant Cell.
640 2017;29(8):1806-21.
641 25. Cole R, Peremyslov V, Van Why S, Moussaoui I, Ketter A, Cool R, et al. A
642 broadly conserved NERD genetically interacts with the exocyst to affect root growth and
643 cell expansion. J Exp Bot. 2018;69(15):3625-37.
644 26. Peaucelle A, Braybrook SA, Le Guillou L, Bron E, Kuhlemeier C, Hofte H. Pectin-
645 induced changes in cell wall mechanics underlie organ initiation in Arabidopsis. Curr
646 Biol. 2011;21(20):1720-6.
647 27. Peaucelle A, Louvet R, Johansen JN, Hofte H, Laufs P, Pelloux J, et al.
648 Arabidopsis phyllotaxis is controlled by the methyl-esterification status of cell-wall
649 pectins. Curr Biol. 2008;18(24):1943-8.
650 28. Barczyk M, Carracedo S, Gullberg D. Integrins. Cell Tissue Res.
651 2010;339(1):269-80.
652 29. Nagpal P, Quatrano RS. Isolation and characterization of a cDNA clone from
653 Arabidopsis thaliana with partial sequence similarity to integrins. Gene. 1999;230(1):33-
654 40.
655 30. Wang G, Ellendorff U, Kemp B, Mansfield JW, Forsyth A, Mitchell K, et al. A
656 genome-wide functional investigation into the roles of receptor-like proteins in
657 Arabidopsis. Plant Physiol. 2008;147(2):503-17.
658 31. He Y, Zhou J, Shan L, Meng X. Plant cell surface receptor-mediated signaling - a
659 common theme amid diversity. J Cell Sci. 2018;131(2).

660 32. Bleckmann A, Weidtkamp-Peters S, Seidel CA, Simon R. Stem cell signaling in
661 Arabidopsis requires CRN to localize CLV2 to the plasma membrane. Plant Physiol.
662 2010;152(1):166-76.
663 33. Brand U, Fletcher JC, Hobe M, Meyerowitz EM, Simon R. Dependence of Stem Cell Fate
664 in Arabidopsis on a Feedback Loop Regulated by CLV3 Activity. Science.
665 2000;289(5479):617-9.
666 34. Zhu Y, Wang Y, Li R, Song X, Wang Q, Huang S, et al. Analysis of interactions among the
667 CLAVATA3 receptors reveals a direct interaction between CLAVATA2 and CORYNE in
668 Arabidopsis. Plant J. 2010;61(2):223-33.
669 35. Abrash EB, Davies KA, Bergmann DC. Generation of signaling specificity in Arabidopsis by
670 spatially restricted buffering of ligand-receptor interactions. Plant Cell. 2011;23(8):2864-79.
671 36. Shpak ED, McAbee JM, Pillitteri LJ, Torii KU. Stomatal patterning and differentiation by
672 synergistic interactions of receptor kinases. Science. 2005;309(5732):290-3.
673 37. Elliott RC, Betzner AS, Huttner E, Oakes MP, Tucker WQ, Gerentes D, et al.
674 AINTEGUMENTA, an APETALA2-like gene of Arabidopsis with pleiotropic roles in ovule
675 development and floral organ growth. The Plant Cell. 1996;8(2):155-68.
676 38. Klucher KM, Chow H, Reiser L, Fischer RL. The AINTEGUMENTA gene of Arabidopsis
677 required for ovule and female gametophyte development is related to the floral homeotic gene
678 APETALA2. The Plant Cell. 1996;8(2):137-53.
679 39. Modrusan Z, Reiser L, Feldmann KA, Fischer RL, Haughn GW. Homeotic Transformation
680 of Ovules into Carpel-like Structures in Arabidopsis. The Plant Cell. 1994;6(3):333-49.
681 40. Robinson-Beers K, Pruitt RE, Gasser CS. Ovule Development in Wild-Type Arabidopsis
682 and Two Female-Sterile Mutants. The Plant Cell. 1992;4(10):1237-49.
683 41. Schneitz K, Hulskamp M, Kopczak SD, Pruitt RE. Dissection of sexual organ ontogenesis:
684 a genetic analysis of ovule development in Arabidopsis thaliana. Development.
685 1997;124(7):1367-76.
686 42. Wilson ZA, Zhang DB. From Arabidopsis to rice: pathways in pollen development. J Exp
687 Bot. 2009;60(5):1479-92.
688 43. Schaller GE, Bishopp A, Kieber JJ. The Yin-Yang of Hormones: Cytokinin and Auxin
689 Interactions in Plant Development. The Plant Cell. 2015;27(1):44-63.
690 44. Rameau C, Bertheloot J, Leduc N, Andrieu B, Foucher F, Sakr S. Multiple pathways
691 regulate shoot branching. Front Plant Sci. 2014;5:741.
692 45. Thimann KV, Skoog F. Studies on the Growth Hormone of Plants: III. The Inhibiting
693 Action of the Growth Substance on Bud Development. Proc Natl Acad Sci U S A. 1933;19(7):714-
694 6.
695 46. Domagalska MA, Leyser O. Signal integration in the control of shoot branching. Nature
696 Reviews Molecular Cell Biology. 2011;12:211.
697 47. Lo SF, Yang SY, Chen KT, Hsing YI, Zeevaart JA, Chen LJ, et al. A novel class of gibberellin
698 2-oxidases control semidwarfism, tillering, and root development in rice. Plant Cell.
699 2008;20(10):2603-18.
700 48. Silverstone AL, Mak PY, Martinez EC, Sun TP. The new RGA locus encodes a negative
701 regulator of gibberellin response in Arabidopsis thaliana. Genetics. 1997;146(3):1087-99.
702 49. Best NB, Hartwig T, Budka J, Fujioka S, Johal G, Schulz B, et al. nana plant2 Encodes a
703 Maize Ortholog of the Arabidopsis Brassinosteroid Biosynthesis Gene DWARF1, Identifying

704 Developmental Interactions between Brassinosteroids and Gibberellins. Plant Physiol.
705 2016;171(4):2633-47.
706 50. Best NB, Johal G, Dilkes BP. Phytohormone inhibitor treatments phenocopy
707 brassinosteroid–gibberellin dwarf mutant interactions in maize. Plant Direct. 2017;1(2).
708 51. Wickson M, Thimann KV. The Antagonism of Auxin and Kinetin in Apical Dominance.
709 Physiologia Plantarum. 1958;11(1):62-74.
710 52. Sachs T, Thimann KV. THE ROLE OF AUXINS AND CYTOKININS IN THE RELEASE OF BUDS
711 FROM DOMINANCE. American Journal of Botany. 1967;54(1):136-44.
712 53. Yin Y, Wang Z-Y, Mora-Garcia S, Li J, Yoshida S, Asami T, et al. BES1 Accumulates in the
713 Nucleus in Response to Brassinosteroids to Regulate Gene Expression and Promote Stem
714 Elongation. Cell. 2002;109(2):181-91.
715 54. Foo E, Bullier E, Goussot M, Foucher F, Rameau C, Beveridge CA. The branching gene
716 RAMOSUS1 mediates interactions among two novel signals and auxin in pea. Plant Cell.
717 2005;17(2):464-74.
718 55. Shimizu-Sato S, Tanaka M, Mori H. Auxin-cytokinin interactions in the control of shoot
719 branching. Plant molecular biology. 2009;69(4):429-35.
720 56. Wang Y, Sun S, Zhu W, Jia K, Yang H, Wang X. Strigolactone/MAX2-induced degradation
721 of brassinosteroid transcriptional effector BES1 regulates shoot branching. Developmental cell.
722 2013;27(6):681-8.
723 57. Huang HY, Jiang WB, Hu YW, Wu P, Zhu JY, Liang WQ, et al. BR signal influences
724 Arabidopsis ovule and seed number through regulating related genes expression by BZR1. Mol
725 Plant. 2013;6(2):456-69.
726 58. Nam YJ, Herman D, Blomme J, Chae E, Kojima M, Coppens F, et al. Natural Variation of
727 Molecular and Morphological Gibberellin Responses. Plant Physiol. 2017;173(1):703-14.
728 59. Vu V, Verster AJ, Schertzberg M, Chuluunbaatar T, Spensley M, Pajkic D, et al. Natural
729 Variation in Gene Expression Modulates the Severity of Mutant Phenotypes. Cell.
730 2015;162(2):391-402.
731 60. Lempe J, Balasubramanian S, Sureshkumar S, Singh A, Schmid M, Weigel D. Diversity of
732 flowering responses in wild Arabidopsis thaliana strains. PLoS Genet. 2005;1(1):109-18.
733 61. Curtis MD, Grossniklaus U. A gateway cloning vector set for high-throughput functional
734 analysis of genes in planta. Plant Physiol. 2003;133(2):462-9.
735 62. Clough SJ, Bent AF. Floral dip: a simplified method for Agrobacterium-mediated
736 transformation of Arabidopsis thaliana. Plant J. 1998;16(6):735-43.
737 63. Davis TC, Jones DS, Dino AJ, Cejda NI, Yuan J, Willoughby AC, et al. Arabidopsis thaliana
738 MLO genes are expressed in discrete domains during reproductive development. Plant Reprod.
739 2017;30(4):185-95.
740 64. Nelson BK, Cai X, Nebenfuhr A. A multicolored set of in vivo organelle markers for co-
741 localization studies in Arabidopsis and other plants. Plant J. 2007;51(6):1126-36.
742 65. Jones DS, Yuan J, Smith BE, Willoughby AC, Kumimoto EL, Kessler SA. MILDEW
743 RESISTANCE LOCUS O Function in Pollen Tube Reception Is Linked to Its Oligomerization and
744 Subcellular Distribution. Plant Physiol. 2017;175(1):172-85.
745 66. Alexander MP. Differential staining of aborted and nonaborted pollen. Stain Technol.
746 1969;44(3):117-22.

747 67. Kumar S, Stecher G, Tamura K. MEGA7: Molecular Evolutionary Genetics Analysis
748 Version 7.0 for Bigger Datasets. Mol Biol Evol. 2016;33(7):1870-4.
749 68. Felsenstein J. Confidence-Limits on Phylogenies - an Approach Using the Bootstrap.
750 Evolution. 1985;39(4):783-91.
751

752

753 **Acknowledgements**

754 We thank Dr. Brian Dilkes, Dr. John Fowler, Dr. Daniel S. Jones, Thomas Davis, Yan
755 Ju, and Rachel Flynn for helpful discussions and comments on the manuscript. We
756 thank Dr. Xutong Wang for help with the statistical analysis. Purdue University Start-up
757 funds and a grant from the Oklahoma Center for the Advancement of Science and
758 Technology #PS14-008 to S.A.K. supported this work.

759

760 **Author contributions**

761 **Conceptualization:** JY SAK.

762 **Data curation:** JY.

763 **Formal analysis:** JY SAK.

764 **Funding acquisition:** SAK.

765 **Investigation:** JY.

766 **Methodology:** JY.

767 **Project administration:** SAK.

768 **Resources:** JY SAK.

769 **Supervision:** SAK.

770 **Validation:** JY.

771 **Visualization:** JY.

Writing – original draft: JY.

Writing – review & editing: JY SAK.

Competing Interests

The authors declare no competing interests.

780 **Figure Legends**

781 **Fig 1. Arabidopsis accessions display natural variation in ovule number per**
782 **flower.** (A) Boxplot of ovule number in 189 Arabidopsis accessions. The detailed names
783 of these accessions are in Supplementary Table 1. (B) Dissected siliques of low,
784 medium, and high ovule number accessions (Bar=2.0mm). (C) Geographic distribution
785 of accessions. Groups 1 to 6 correspond to ovule number ranking (from low to high),
786 with the colors corresponding to panel A. The pie chart indicates the percentage of
787 accessions in each country in each ovule number group, while the size of the pie chart
788 corresponds to the total number of accessions per country. (D) Cladogram of
789 accessions used in this study (generated in MEGA7). The 15 accessions labeled in blue
790 had the lowest ovule numbers, and the 15 accessions labeled with red had the highest
791 ovule numbers. The arrow points to a clade with clustered low ovule number
792 accessions.

793

794 **Fig 2. GWAS identifies candidate loci associated with ovule number per flower.**
795 (A) Manhattan plot for the SNPs associated with ovule number per flower.
796 Chromosomes are depicted in different colors. The horizontal blue dashed line
797 corresponds to a $-\log_{10}(p \text{ values}) \geq 6.2$ and the red dashed line corresponds to $-\log_{10}(p$
798 $\text{values}) \geq 7.5$ after Benjamini Hochberg (False Discovery Rate) correction. (B) The
799 genomic region surrounding the two most significant GWA peaks on Chromosome 3.
800 (C) Genes in the genomic region surrounding the two significant GWA peaks in (D). The
801 red boxes are AT3G51050 (*NERD1*) and AT3T60660 (*ONA2*).

802

803 **Fig 3. *nerd1* mutants have reduced fertility.** (A) Bar graph of ovule number per flower
804 in Col-0, *nerd1-2*, *nerd1-4* and their complementation lines. "***" indicates statistical
805 significance (*p* value<0.001 determined by Student's t-test). (B-C) *nerd1-2/nerd1-2*
806 displays lower ovule number, infertile ovules, and short siliques compared to Col-0 and
807 complemented lines. (D) Alexander stained Col-0 anthers have viable pollen grains (red
808 indicates viable pollen while the green is non-viable). (E) Alexander-stained *nerd1-*
809 *2/nerd1-2* anthers have no viable pollen. (F) Col-0 mature ovule with a normal embryo
810 sac. (G) *nerd1-2/nerd1-2* mature ovule with an aborted embryo sac. Bars=2.5mm (B-C),
811 20µm (D-G).
812
813 **Fig 4. NERD1 is conserved across plant lineages.** (A) Phylogenetic tree from amino
814 acid alignment of NERD1 generated using the Neighbor-joining method in MEGA7. (B)
815 NERD1 alignment showing sequence conservation among species. The green boxes
816 correspond to conserved regions of NERD1 and the lines represent gaps in the
817 alignment. The red box indicates the FG-GAP domain annotated in NERD1 by
818 Langhans, et al., 2017.
819
820 **Fig 5. NERD1 co-localizes with a Golgi marker in *N. benthamiana* epidermal cells.**
821 (A) NERD1 protein domains determined by TMHMM 2.0. (B) NERD1-GFP (green
822 signal) co-localizes with Golgi-mCherry (magenta signal) in *N. benthamiana* epidermal
823 cells. (C) NERD1-GFP (green signal) does not co-localize with ER-mCherry (magenta
824 signal). (D) NERD1-GFP (green signal) partially co-localizes with PM-mCherry
825 (magenta signal). Bars=15 µm.

826

827 **Fig 6. NERD1 expression in plant development.** The NERD1$_{pro}$::NERD1-GUS
828 reporter (blue signal) is detected in inflorescence (A-B), the flower in stage 9 (C), the
829 pistil in stage 8 (D), the pistil in stage 9 (E), mature pistil (F), mature flower (G), mature
830 anther (H), and SAM and RAM of seedlings (I). Bars=25 μm.

831

832 **Fig 7. NERD1 expression is reduced in developing flowers of a low ovule number**
833 **accession.**
834 (A) qRT-PCR of NERD1 in Col-0 and Altai-5 inflorescences. (B) qRT-PCR of NERD1 in
835 Col-0 and Altai-5 leaves. "***" indicates statistical significance at *p* value<0.001
836 determined by Student's t-test.

837

838 **Fig 8. Overexpression of NERD1 affects plant architecture and fertility.** (A-B)
839 35S::NERD1-GFP expressed in Col-0 and Altai-5 backgrounds. Bars=5cm. Bar graphs
840 of total ovule number per flower (C), total branch number (D), total flower number per
841 plant (E), number of flowers within 15 cm of the main shoot (F), and distance between
842 adjacent flowers (G-H) in 35S::NERD1-GFP transformants in the Col-0 and Altai-5
843 backgrounds compared to untransformed controls.

844

845 **Fig 9. Sequence variation in the *NERD1* locus correlates with ovule number.** (A)
846 SNPs in and around the *NERD1* gene. The blue line indicates the 16 lowest ovule
847 number accessions and the red line indicates the 16 highest ovule number accessions.
848 SNPs are identified based on comparison to the Col-0 reference genome. The red

849 boxes highlight low-ovule number associated SNPs (the turquoise bar indicates two
850 SNPs in adjacent nucleotides, a non-synonymous C-A SNP and a synonymous C-G
851 SNP). Only genomes that were available on the SALK 1,001 genomes browser
852 (http://signal.salk.edu/atg1001/3.0/gebrowser.php) were considered. (B) One of the
853 ovule number-associated SNPs in NERD1 causes a serine-tyrosine substitution in low
854 ovule number accessions. (C) Average ovule number in *NERD1* “A” and “C” allele-
855 containing accessions. The “A” allele is significantly associated with lower ovule
856 numbers. “***” indicates statistical significance at p value<0.001 determined by
857 Student’s t-test.
858

Figure 1

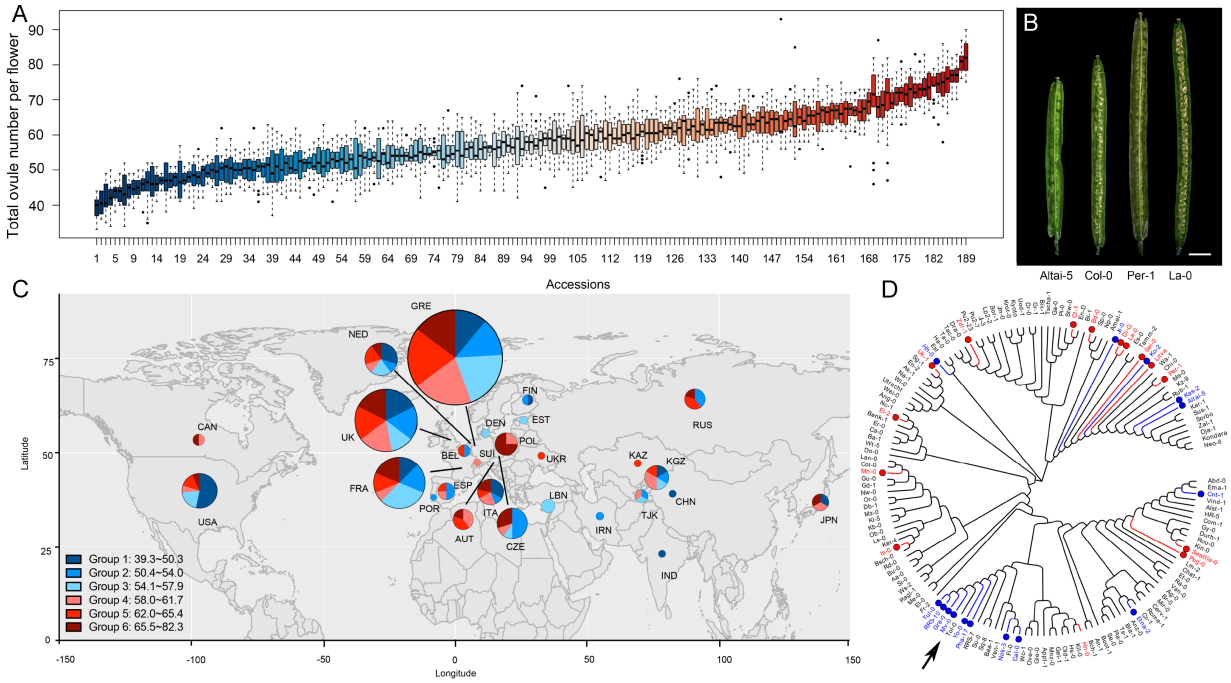

Fig 1. Arabidopsis accessions display natural variation in ovule number per flower. (A) Boxplot of ovule number in 189 Arabidopsis accessions. The detailed names of these accessions are in Supplementary Table 1. (B) Dissected siliques of low, medium, and high ovule number accessions (Bar=2.0mm). (C) Geographic distribution of accessions. Groups 1 to 6 correspond to ovule number ranking (from low to high), with the colors corresponding to panel A. The pie chart indicates the percentage of accessions in each country in each ovule number group, while the size of the pie chart corresponds to the total number of accessions per country. (D) Cladogram of accessions used in this study (generated in MEGA7). The 15 accessions labeled in blue had the lowest ovule numbers, and the 15 accessions labeled with red had the highest ovule numbers. The arrow points to a clade with clustered low ovule number accessions.

Figure 2

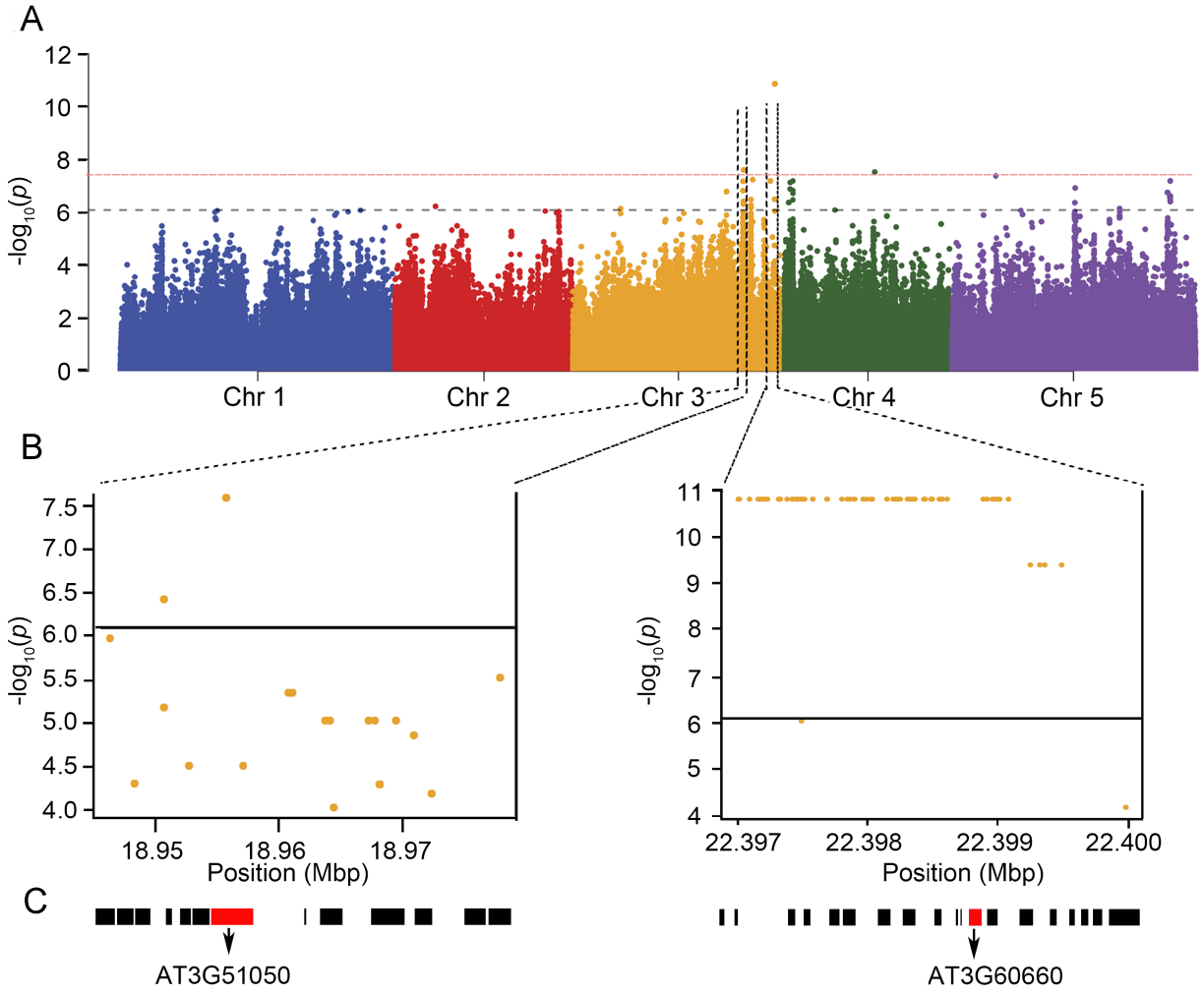

Fig 2. GWAS identifies candidate loci associated with ovule number per flower. (A) Manhattan plot for the SNPs associated with ovule number per flower. Chromosomes are depicted in different colors. The horizontal blue dashed line corresponds to a $-\log_{10}(p \text{ values}) \geq 6.2$ and the red dashed line corresponds to $-\log_{10}(p \text{ values}) \geq 7.5$ after Benjamini Hochberg (False Discovery Rate) correction. (B) The genomic region surrounding the two most significant GWA peaks on Chromosome 3. (C) Genes in the genomic region surrounding the two significant GWA peaks in (D). The red boxes are AT3G51050 (*NERD1*) and AT3T60660 (*ONA2*).

Figure 3

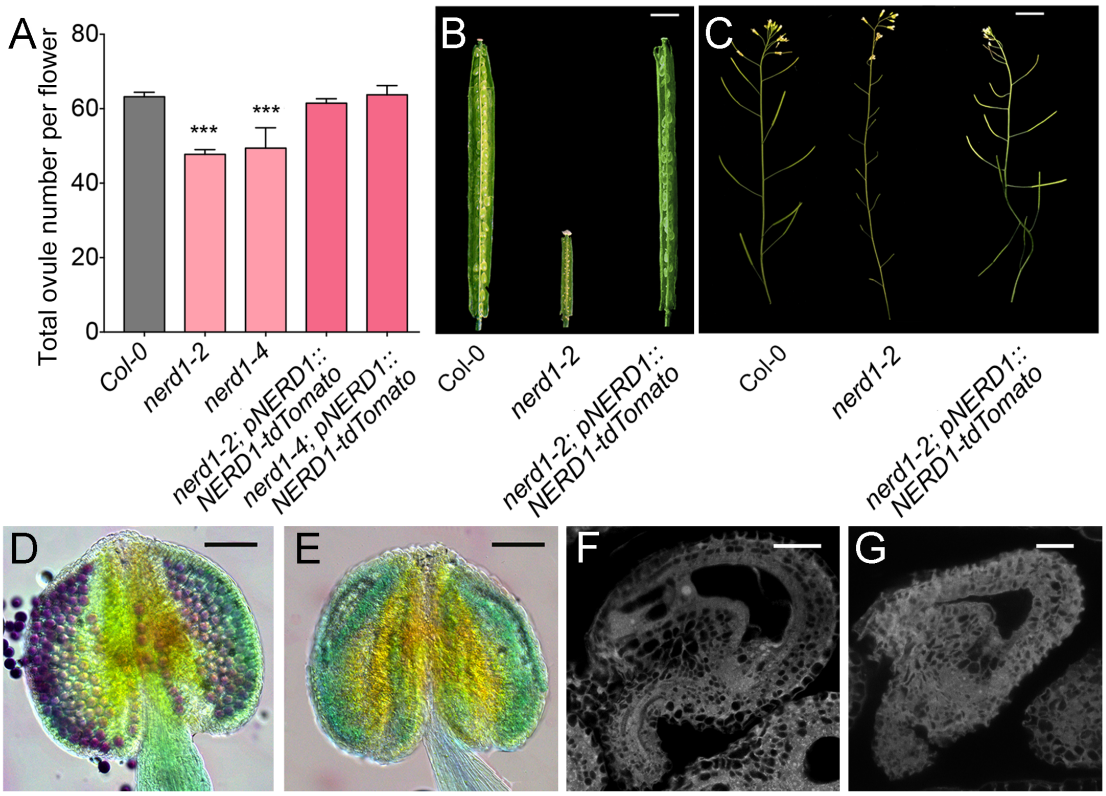

Fig 3. *nerd1* mutants have reduced fertility. (A) Bar graph of ovule number per flower in Col-0, *nerd1-2*, *nerd1-4* and their complementation lines. "***" indicates statistical significance (*p* value<0.001 determined by Student's t-test). (B-C) *nerd1-2/nerd1-2* displays lower ovule number, infertile ovules, and short siliques compared to Col-0 and complemented lines. (D) Alexander stained Col-0 anthers have viable pollen grains (red indicates viable pollen while the green is non-viable). (E) Alexander-stained *nerd1-2/nerd1-2* anthers have no viable pollen. (F) Col-0 mature ovule with a normal embryo sac. (G) *nerd1-2/nerd1-2* mature ovule with an aborted embryo sac. Bars=2.5mm (B-C), 20µm (D-G).

Figure 4

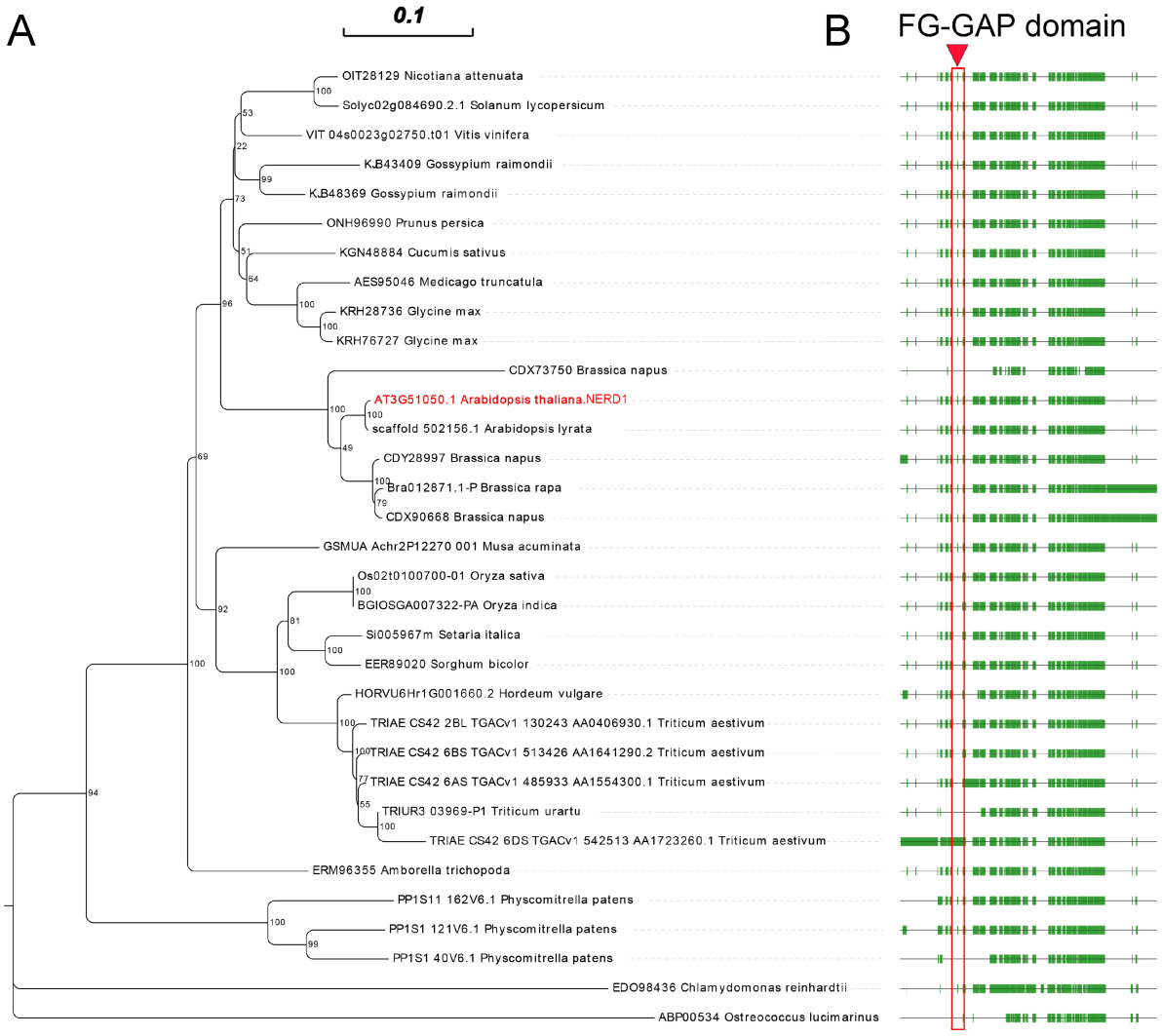

Fig 4. NERD1 is conserved across plant lineages. (A) Phylogenetic tree from amino acid alignment of NERD1 generated using the Neighbor-joining method in MEGA7. (B) NERD1 alignment showing sequence conservation among species. The green boxes correspond to conserved regions of NERD1 and the lines represent gaps in the alignment. The red box indicates the FG-GAP domain annotated in NERD1 by Langhans, et al., 2017.

Figure 5

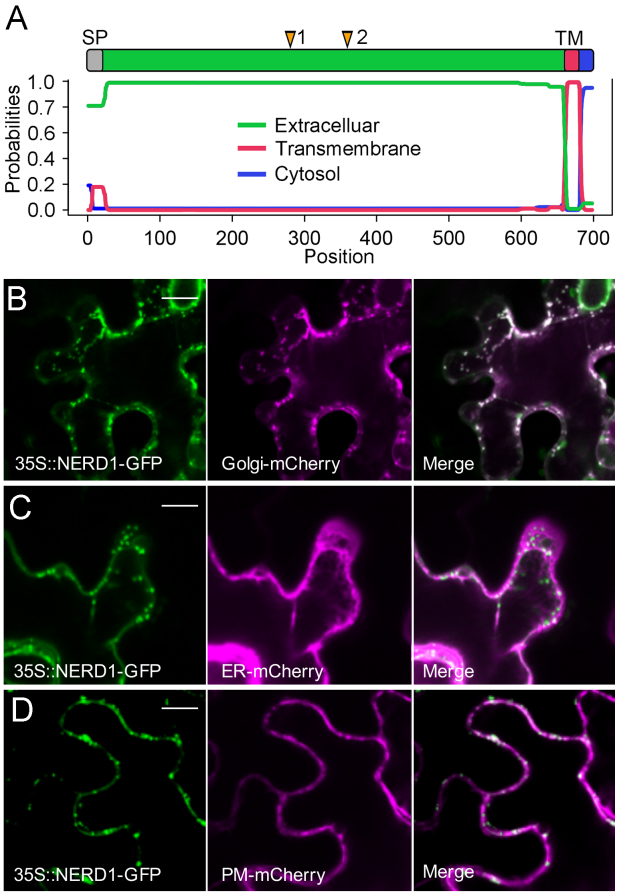

Fig 5. NERD1 co-localizes with a Golgi marker in *N. benthamiana* epidermal cells. (A) NERD1 protein domains determined by TMHMM 2.0. (B) NERD1-GFP (green signal) co-localizes with Golgi-mCherry (magenta signal) in *N. benthamiana* epidermal cells. (C) NERD1-GFP (green signal) does not co-localize with ER-mCherry (magenta signal). (D) NERD1-GFP (green signal) partially co-localizes with PM-mCherry (magenta signal). Bars=15 μm.

Figure 6

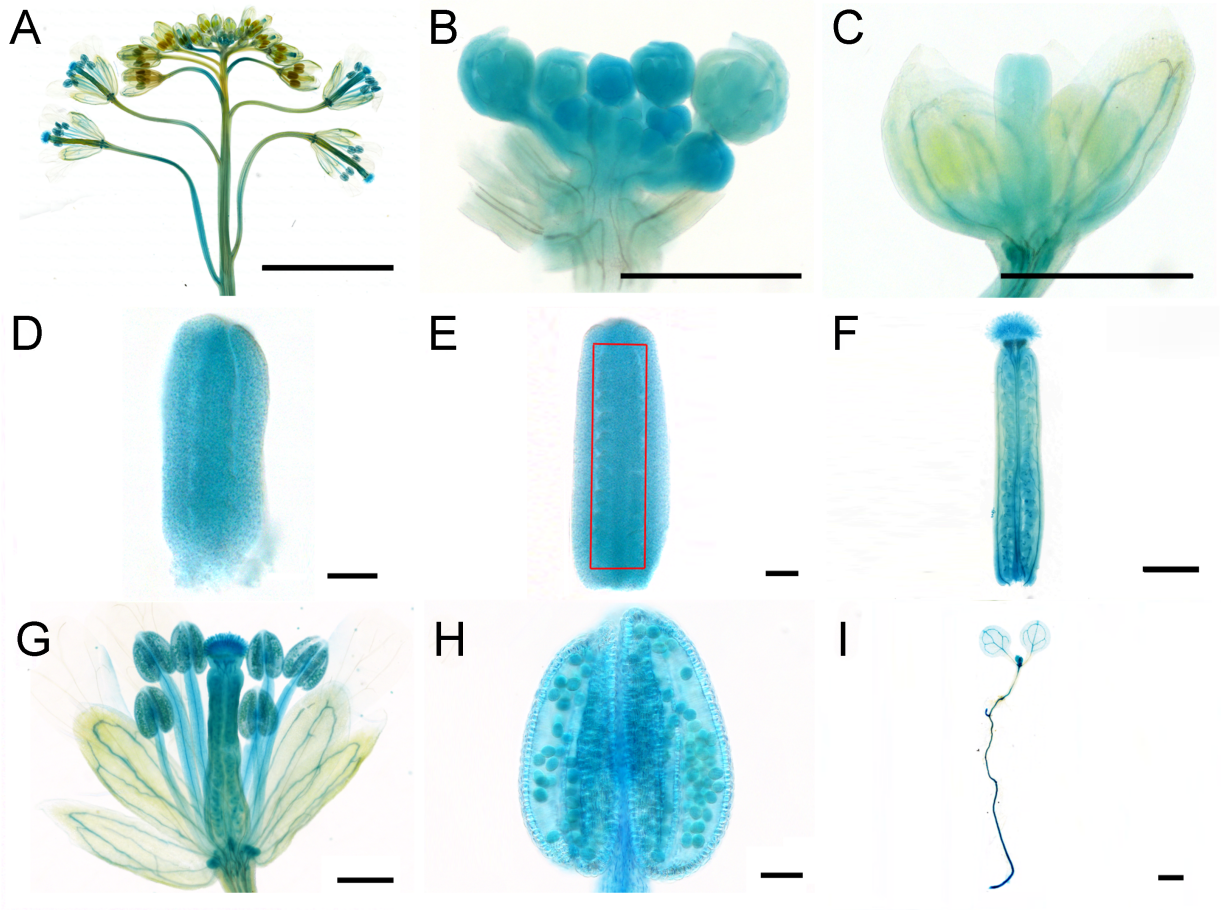

Fig 6. NERD1 expression in plant development. The NERD1$_{pro}$::NERD1-GUS reporter (blue signal) is detected in inflorescence (A-B), the flower in stage 9 (C), the pistil in stage 8 (D), the pistil in stage 9 (E), mature pistil (F), mature flower (G), mature anther (H), and SAM and RAM of seedlings (I). Bars=25 μm.

Figure 7

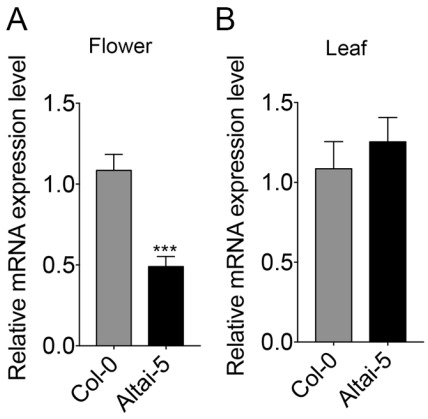

Fig 7. NERD1 expression is reduced in developing flowers of a low ovule number accession. (A) qRT-PCR of NERD1 in Col-0 and Altai-5 inflorescences. (B) qRT-PCR of NERD1 in Col-0 and Altai-5 leaves. "***" indicates statistical significance at *p* value<0.001 determined by Student's t-test.

Figure 8

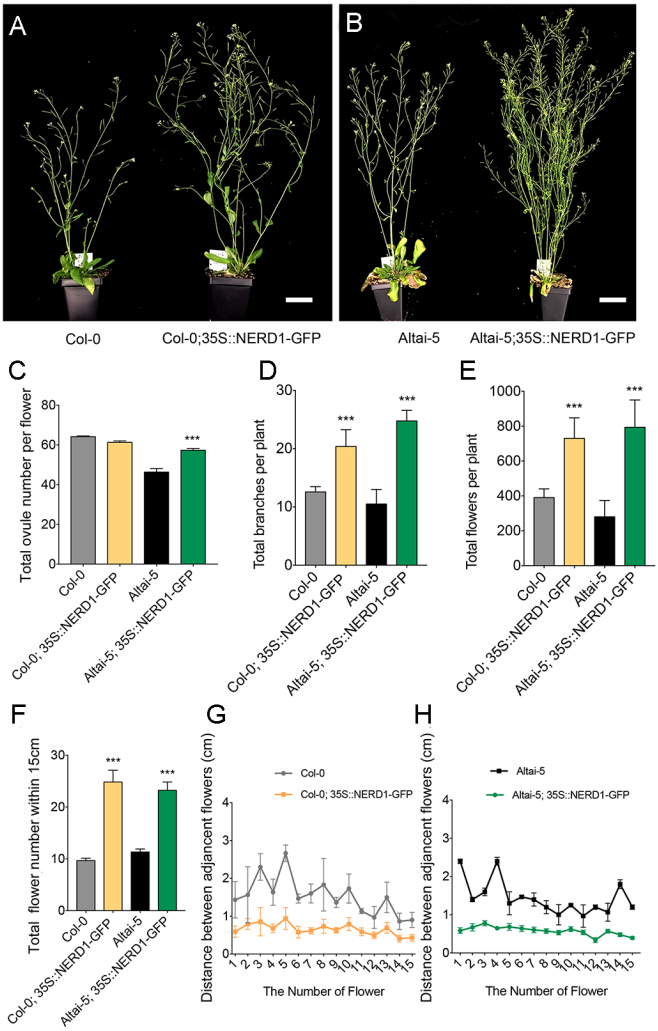

Fig 8. Overexpression of NERD1 affects plant architecture and fertility. (A-B) 35S::NERD1-GFP expressed in Col-0 and Altai-5 backgrounds. Bars=5cm. Bar graphs of total ovule number per flower (C), total branch number (D), total flower number per plant (E), number of flowers within 15 cm of the main shoot (F), and distance between adjacent flowers (G-H) in 35S::NERD1-GFP transformants in the Col-0 and Altai-5 backgrounds compared to untransformed controls.

Figure 9

A

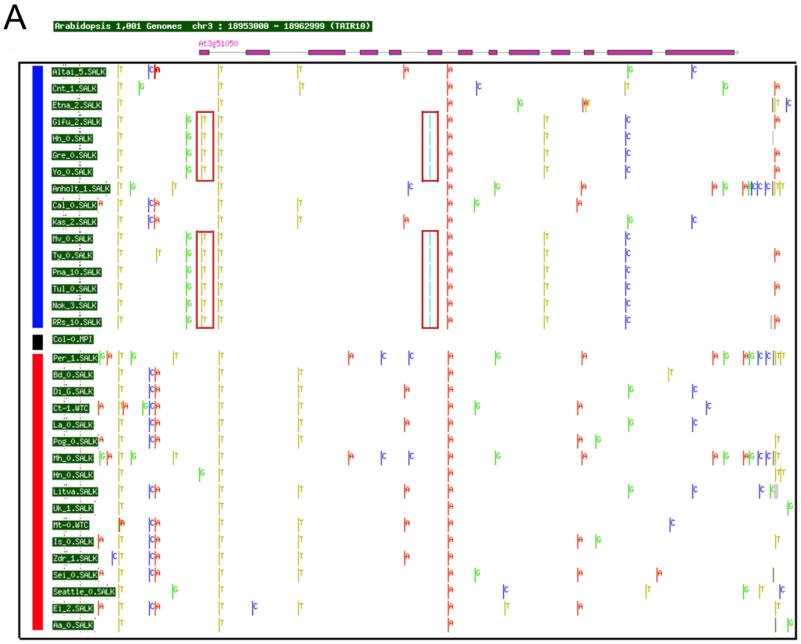

B

Position	*p* value	Alleles	Amino	LOCN
18954034	9.55E-07	C-T	R4	Exon
18955603	2.45E-08	C-A	S230Y	Exon
18955604	2.45E-08	T-C	S230	Exon

C

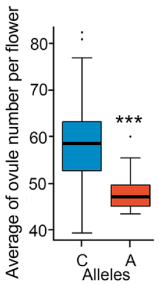

Fig 9. Sequence variation in the *NERD1* locus correlates with ovule number. (A) SNPs in and around the *NERD1* gene. The blue line indicates the 16 lowest ovule number accessions and the red line indicates the 16 highest ovule number accessions. SNPs are identified based on comparison to the Col-0 reference genome. The red boxes highlight low-ovule number associated SNPs (the turquoise bar indicates two SNPs in adjacent nucleotides, a non-synonymous C-A SNP and a synonymous C-G SNP). Only genomes that were available on the SALK 1,001 genomes browser (http://signal.salk.edu/atg1001/3.0/gebrowser.php) were considered. (B) One of the ovule number-associated SNPs in NERD1 causes a serine-tyrosine substitution in low ovule number accessions. (C) Average ovule number in *NERD1* “A” and “C” allele-containing accessions. The “A” allele is significantly associated with lower ovule numbers. “***” indicates statistical significance at *p* value<0.001 determined by Student’s t-test.